Analyst

Accepted Manuscript

ROYAL SOCIETY OF CHEMISTRY

www.rsc.org/analyst

Cite this: DOI: 10.1039/c0xx00000x

www.rsc.org/xxxxxx

ARTICLE TYPE

Nanoscale pillar arrays for separations†

Teresa B. Kirchner[a], Rachel B. Strickhouser[a], Nahla A. Hatab[a], Jennifer J. Charlton[a,b], Ivan I. Kravchenko[c], Nickolay V. Lavrik[c], and Michael J. Sepaniak[*,a]

Received (in XXX, XXX) Xth XXXXXXXXX 20XX, Accepted Xth XXXXXXXXX 20XX

DOI: 10.1039/b000000x

The work presented herein evaluates silicon nano-pillar arrays for use in planar chromatography. Electron beam lithography and metal thermal dewetting protocols were used to create nano-thin layer chromatography platforms. With these fabrication methods we are able to reduce the size of the characteristic features in a separation medium below that used in ultra-thin layer chromatography; i.e. pillar heights are 1-2µm and pillar diameters are typically in the 200-400nm range. In addition to the intrinsic nanoscale aspects of the systems, it is shown they can be further functionalized with nanoporous layers and traditional stationary phases for chromatography; hence exhibit broad-ranging lab-on-a-chip and point-of-care potential. Because of an inherent high permeability and very small effective mass transfer distance between pillars, chromatographic efficiency can be very high but is enhanced herein by stacking during development and focusing while drying, yielding plate heights in the nm range separated band volumes. Practical separations of fluorescent dyes, fluorescently derivatized amines, and anti-tumor drugs are illustrated. Introduction

When used as planar chromatography separations platforms, periodic and stochastic nanoscale pillar arrays are shown to offer attributes of rapid mass transport, high chromatographic efficiency that is influenced by development and post development processes, portability, and diminutive mobile phase and sample requirements. Using clean room fabrication techniques, nano-scale pillar arrays can be fabricated for use as nano-thin layer chromatographic (NTLC) platforms (Figure 1). As dicussed previously,[1, 2] Electron beam lithography (EBL) permits exquisite control of pillar placement and dimensions to form deterministic pillar arrays (herein, DPA). While the highly ordered systems afforded by this lithography method may be ideal in evaluating effects of changes in pillar dimensions on flow characteristics and furthermore separation efficiency, the EBL process requires expensive equipment and is a slow serial process, the combination creates practical limits as to the size and quantity of fabricated arrays. A far more accesssible approach involves fabrication of stochasitc pillar arrays (SPA) using the thermal dewetting of thin Pt films to create masks [1, 3]. Although these SPA systems do not deliver precise control of pillar morphology, placement, and dimensions, previous work has shown,[1] some control is maintained by varying the Pt film thickness. The SPA systems fabricated and evaluated within this work were tailored, as afforded by the method, to as closely approximate the more dense EBL system. Discussed previously,[1] both the EBL and dewetted Pt fabrication methods are capable of creating pillar arrays with dimensions larger and smaller than the platforms reported herein. These dimensions were partially chosen to create the lowest volume platform while minimizing evaporation and keeping the pillars under a 10:1 aspect ratio to maintain robustness and minimize wicking and spotting damage. In this research we study solvent and analyte transport, chromatographic efficiency, and demonstrate chemically selective separations with DPA- and SPA-NTLC platforms.

Desmet et al. has shown that porous silicon adequately increases surface area in ordered arrays to be used as a liquid chromatography platform for systems that are confined and pressurized [4-7]. Previous research from our group has shown that highly ordered pillar arrays prepared by photolithography in the low µm regime, and coated with a thin layer of silicon oxide, functionalized with a carbon reverse stationary phase

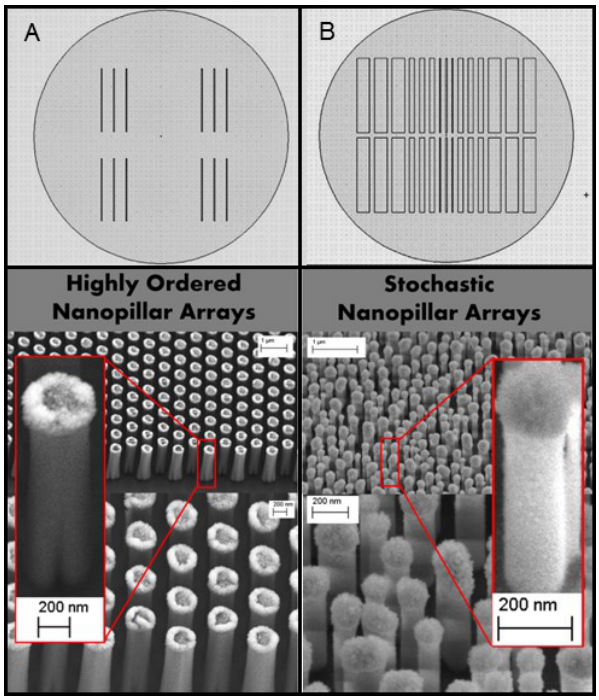

Figure 1: Wafer layout and SEM images of **(A)** DPA and **(B)** SPA patterned NTLC platforms.

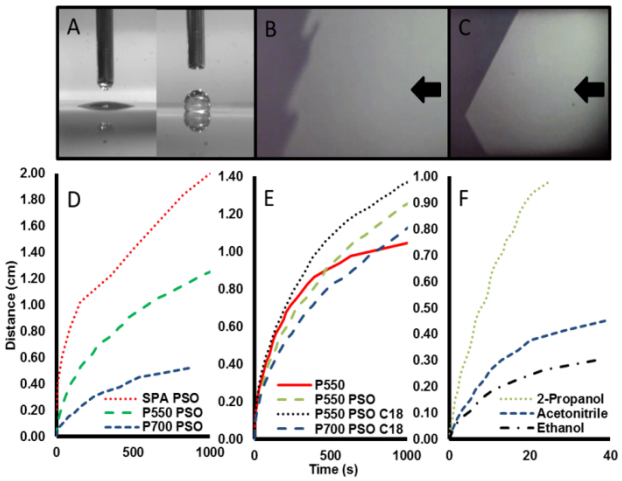

Figure 2: Microscopy images of **(A)** water contact angle on non-functionalized PSO (left) and RP functionalized PSO (right), **(B)** solvent front (direction denoted by arrow) at high velocity early in development, and **(C)** the front as velocity decreases later in development (DPA case). Velocity plots; **(D)** comparing DPA pitch variations, P550 with PSO versus P700 with PSO and comparing DPA versus SPA (pillar diameter ~ 200 nm & pitch ~ 550 nm for the SPA PSO case), **(E)** comparing non-PSO (P550) versus PSO (P550 PSO) DPA and comparing non-functionalized (P550 PSO) versus RP functionalized (P550 PSO C18) and finally comparing pitch with the C18 RP case (550nm versus 700nm). **(D)** and **(E)** use benzyl alcohol while **(F)** uses more traditional solvents for a DPA (P700 PSO C18) system.

(RP), produced plate heights (H) as low as 0.8 µm in closed pressurized array systems[8] and plate heights on average of 2 µm for capillary-action driven open array systems[9]. Combining previously mentioned fabrication protocols followed by reactive ion etching with a room temperature plasma enhanced chemical vapor deposition process creates a conformal porous silicon oxide (PSO) layer on the pillar surface (Figure 1) [10, 11]. These unique arrays create a nano-scale platform for RP chromatographic separations. Increasing the accessible surface area of the system and generating substantial surface silanols for bonding with a C18 RP stationary phase (fabrication details in Supporting Information), ultimately achieve an adequate analyte retention .

In our previous pillar array based ultra-thin layer chromatography (UTLC) work we demonstrated that there is an improved H due to a lack of eddy diffusion (ordered arrays) and minimized resistance to mass transfer in the mobile phase (small pillar diameters and inter pillar gaps)[9]. Equally important was a favorable permeability constant (K_0) or these highly ordered systems, avoiding the adverse effects of small packing particles that are observed in traditional TLC, principally slow flow and a concomitant increase in molecular diffusion broadening of spots. This research was designed to investigate if these trends in flow and H will continue as dimensions are further reduced. It is anticipated that a further reduction in H could occur for these nano-scale systems due to a reduction in feature size as discussed in our previous publications [8, 9, 12, 13], but only if wicking flow is adequate. Further discussion of this topic using the Van Deemter Equation is in Supporting Information.

Additionally, we employed a semi-empirical model developed by Mai et al. for ordered arrays of silicon pillars[13]. This model derived theoretical wicking velocities for varying pillar dimensions. These velocities allowed us to evaluate the effect of pillar hieght, diameter, and pitch and make a predicted efficiency. These predicted values further directed substrate development. The Mai model is based on the geometrical parameters of the fabricated substrate, experimentally measured solvent-substrate contact angles, and literature values for solvent viscosity and surface tension. We then predict H for these nano-scale arrays using a typical diffusion coefficients and the modeled velocity for acetonitrile. This yielded values less than 0.5 µm for the NTLC DPA systems, smaller than the H values observed for UTLC systems reported in our previous work[9]. While the flow model does not consider the porous SiO_2 layer and thus only roughly mimics the experiment, this treatment does motivate scaling down into the nano-regime (further information is found in Supporting Information).

Solvent velocity studies on NTLC platforms

Rapid flow is essential in generating high efficiency separation platforms for separations. Equation [1] describes the effects of parameters on flow in traditional planar chromatography. In this equation, μ_f is the

$$\mu_f^2 = K_0 t d_p \left(\frac{\gamma}{\eta}\right) \cos\theta \qquad [1]$$

displacement of the solvent front, d_p is the diameter of the stationary phase particles, γ represents the surface tension, η the dynamic viscosity and θ, is the contact angle of the mobile phase. The dimensions of the 5 cases investigated (with and without PSO and both types of arrays; DPA and SPA) are summarized in SI Table 1.

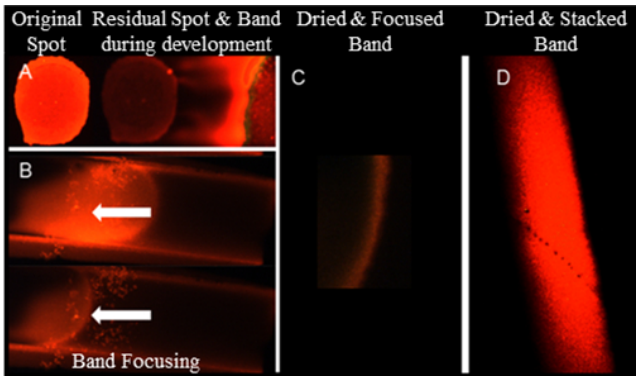

Figure 3: Illustration of processes that influence the dispersion (or concentrating) of initially spotted samples of SR640. **(A)** and **(B)** are imaged with mobile phase (ethanol: water & benzyl alcohol) present while **(C)** and **(D)** are dried cases. In **(A)** the solvation of the initial spot exhibits a concentrating effect (400 µm wide DPA, likewise **B & C). (B)** demonstrates the focusing effect as the solvent (benzyl alcohol) evaporates (note arrows in same position top and bottom). Demonstrated in **(C)** and **(D)** are dried bands that are *focused* (400 µm wide DPA, benzyl alcohol), H~100nm (n=3) and *stacked* (SPA, ethanol:water), H~900nm, respectively.

Varying pitch is ideal for this study because, for these pillar array systems, the interpillar gap behaves as particle diameter (d_p from Equation 1) in traditional planar chromatography systems. Figure 2 illustrates typical solvent behavior for these nanoscale systems. Figure 2A shows the contact angle of water on PSO on flat silicon before (left) and after (right) functionalization with the C18 RP. The hydrophobic character of the surface indicates successful RP functionalization. Figures 2B and 2C are comparisons of the acetonitrile solvent front where the blurriness in the former is probably due to very rapid wicking early in development. These images show pinning behavior at the solvent front. This behavior self-adjusts during development and should not affect bands significantly behind the solvent front. Due to noticeable evaporation issues with traditional RP mobile phases (Figure 2F) we used benzyl alcohol as a low vapor pressure mobile phase in experiments that allowed us to identify effects of the pillar array design parameters on their wicking characteristics. In particular, we analyzed how presence of a PSO coating, pitch and degree of order in the arrays affected the observed wicking velocity (Figures 2D and 2E). Solvent properties are in Supporting Information SI Table 2.

The results of this analysis show that as the pitch decreases the solvent velocity increases (Figure 2D, P550 PSO vs P700 PSO). When comparing the SPA to the ordered DPA systems, the former exhibits significantly faster wicking (Figure 2D). A possible explanation for this behavior may be found in the law of flow resistance in parallel channels as discussed previously for SPA systems[1, 14, 15]. Figure 2E compares the PSO to the non-PSO arrays. It shows that the solvent velocity is greater as distance increases when compared to the non-PSO for the DPA case. Also, it was observed that the solvent front traveled a greater distance with the addition of PSO. These observations may be due to an increase in nano-capillaries and surface area, the latter benefits chromatographic retention, on the PSO modified surface [16-19]. Figure 2F is a comparison of the behavior of more traditional RP solvents. The resulting data cannot be explained by Equation [1] alone, which predicts the wicking velocities in the following order: acetonitrile > ethanol > 2-propanol. This discrepancy is most likely due to effects of more pronounced evaporation of more volatile solvents from the surface of the shallow NTLC platforms.

NTLC patform efficiency analysis

The H treatment that was used as a predictive exercise to validate the premise for this research was based on the well-known work reported by Guiochon[20] and is often used in planar chromatography. Further discussion of this treatment can be found in Supporting Information.

In terms of chromatographic efficiency, evaporation reduces net flow (Figure 2F) for these nano-scale systems, especially as the development proceeds and, as a consequence, molecular diffusion can become problematic as is the case in traditional TLC. The flow of benzyl alcohol is slow due to an unfavorable γ/η ratio whereas for acetonitrile, with a favorable ratio, the model-predicted flow (see Supporting Information SI Figure 2) is much greater than experimentally observed, presumably due to evaporation.

In spite of these issues with solvent velocity and evaporation the observed efficiencies in our system under different mobile phase conditions as shown in Figure 3 and 4 are better than expected. We contend that the traditional Van Deemter

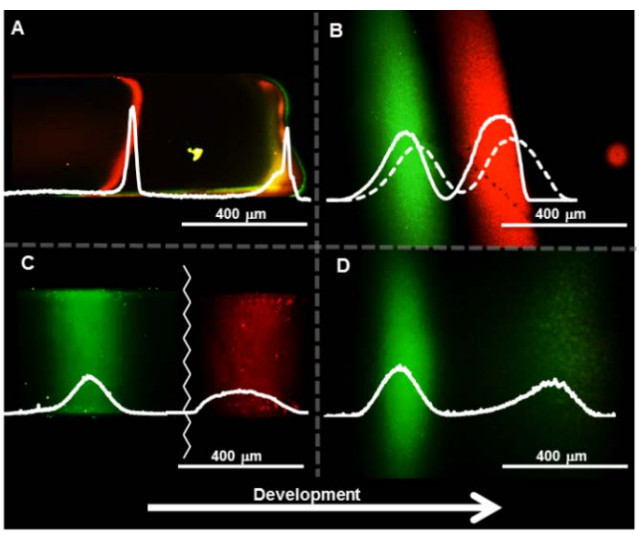

Figure 4: Illustration of separations using DPA (P450G125) **(A)** and **(C)** and SPA (P227G414) **(B)** and **(D)** each with 25nm PSO and C18. **(A)** separation of fluorescent dyes SR 640 (more retained) and FITC (at solvent front), **(B)** separation of dyes coumarin 102 (more retained) and SR640, **(C)** separation of anti-tumor drugs D_1 (more retained) and A_1, and **(D)** separations of fluorescently-derivatized environmental amines n-heptyl amine (more retained) and n-propyl amine. In **(A)** slow drying benzyl alcohol is employed as the mobile phase on an array that resulted in very little retention, substantial focusing (H ~ 25 nm) occurs. Conversely, the other separations are performed with **(B)** ethanol, 80%, **(C)** 2-propanol, 60%,and **(D)** ethanol, 70% all in un-buffered water. Chromatographic traces were generated using Image J 1.47V.

efficiency variables give way to fortuitous beneficial effects of *stacking* during development and *focusing* while drying. For these studies less band dispersion in the direction of the solvent direction was observed. For example, consider the aspect ratio of the band seen in Figures 3D, 4B & 4D. We propose a stacking phenomenon caused by a gradient of the phase ratio (β = volume mobile phase/volume stationary phase) occurs in the direction of flow during the development. This implies that the phase ratio at the front of the band is smaller than at the tail of the band causing a spatial contraction. Such effects are well known in TLC [21-25], however the scale of the NTLC system is likely to exacerbate the phase ratio issue. When mixed solvents are used uneven evaporation can also play a role. Although, ideally, we aim to minimize evaporation, there are unique positive effects shown in this work. Additional observations include a degree of curvature across the band of the DPA (Figure 4A). Contributions to this phenomena include solvent considerations (curvature increases when the band is at or near the solvent front) as well as effects of the morphological heterogeneity of the system at the array boundry (see Figure 3 in Supporting Information).

It is also important that as the solvent interacts with the initial dried spot, slow solvation kinetics, as described by Poole[24], does not contribute to band broadening. Figure 3A shows that a concentrating effect is observed as the solvent interacts with the dried spot (note also the image of the pillar top residual after the front passes). While discrete concentrating zones have been implemented in UTLC platforms that also produce concentrating effects[26] our NTLC platforms are morphologically homogeneous (except for at the array boundaries), although there could be an element of overloading contributing to the effect observed in the figure. Although not done herein, discrete concentrating zones (e.g., thicker PSO layers) could be fabricated into our NTLC platforms as well.

A second type of concentrating effect is focusing of the band after development as the band dries (Figure 3B). The focusing effect is occurring from the solvent front towards the origin. It should be noted that the concentration of the sulforhodamine 640 (SR640) necessary to image the development in rapid real time in Figures 3A and 3B was high and is most likely overloading the array and, also, the fluorescence intensity is enhanced by the solvent in comparison to the dry cases (Figure 3C & 3D). The focusing effect appears to be solvent dependent in that it has only been observed while using solvents that are viscous and have very low vapor pressure and hence dry relatively slowly. The calculated efficiencies (H) in Figure 3D (stacking case) and Figure 3C (focusing case) are approximately 900nm, peak capcacity > 50, and 100nm, peak capacity >150 (n=3), respectively (methods to compute H and approximate peak capacity appear in Supporting Information). Although it is tempting to equate this focusing with direct coffee ring effects[27, 28], it is noteworthy that the dynamics of evaporation of solute containing bands in this work involve a surface with multiple layers of roughness and a partition capacity for the analyte. Stacking and focusing are discussed further in Supporting Information. Focusing and stacking effects are most likely R_f dependent, however, other contributing factors to these effects should be investigated to determine if the processes can be tuned and controlled to maximize resolution. The narrower bandwidth shown in Figure 3 C versus D is not indicative that DPA are superior to SPA, but rather indicates the increase in efficiency observed in the case of focusing effects. A more thorough discussion on the focusing and stacking effects can be found in Supporting Information.

NTLC patform separations

The potential of the NTLC platforms for significant, extremely low volume separations was evaluated. Figures 4A and 4B are separations of standard dyes on DPA (sulforhodamine 640 (SR640) and fluorescein isothiocyanate (FITC)) and SPA (SR640 and coumarin 102) platforms, respectively. Figure 4C is a separation of the anti-tumor drugs Daunorubicin (D_1) and Adriamycin (A_1) on a DPA and Figure 4D is a separation of fluorescently derivatized environmental amines, 7-nitrobenz-2-oxa-1,3-diazole (NBD)- n-heptyl and n-propyl amine on a SPA. Note that resolution is enhanced (e.g. in Figure 4B) due to stacking effects and, when generating chromatograms, selecting the central 25% of the stacked band (solid) also improves resolution relative to using the entire band (dashed). In addition to baseline resolution for these separations, plate heights are less than 1 µm and band volumes are in the pL range.

Conclusions

We demonstrate herein the fabrication of DPA- and SPA-NTLC platforms that can be made into porous shell-core structures and surface modified with hydrophobic character. The arrays share traits for separations of more traditional approaches but are truly nano in scale and offer attributes of systems at that scale. In particular, NTLC is shown to behave uniquely in terms of solvent and analyte spot transport and dispersion, producing extremely low volume separations with high efficiency. While issues involving solvent evaporation were observed, it is expected that they can be overcome with further research.

Acknowledgements

This material is based upon work supported by the National Science Foundation under Grant No. 1144947 with the University of Tennessee, Knoxville. A portion of this research was conducted at the Center for Nanophase Materials Sciences, which is sponsored at Oak Ridge National Laboratory by the Scientific User Facilities Division, Office of Basic Energy Sciences, U.S. Department of Energy.

We also acknowledge John R. Dunlap, Ph.D., and the JIAM Microscopy Center and Advanced Microscopy and Imaging Center at UTK for access to facilities.

Notes and references

[a] *Department of Chemistry, University of Tennessee, Knoxville, TN, 37996, USA.*

[b] *Y-12 National Security Complex, Analytical Chemistry Organization, Oak Ridge, TN 37830, USA*

[c] *Center for Nanophase Materials Sciences, Oak Ridge National Laboratory, Oak Ridge, TN, 37830, USA.*

† Electronic Supplementary Information (ESI) available:

1. J. J. Charlton, N. Lavrik, J. A. Bradshaw and M. J. Sepaniak, *ACS Applied Materials & Interfaces*, 2014.
2. D. M. Tennant, *journal of Vacuum Science Technology*, 2013, 31.
3. R. L. Agapov, B. Srijanto, C. Fowler, D. Briggs, N. V. Lavrik and M. J. Sepaniak, *Nanotechnology*, 2013, 24, 505302-505311.
4. D. Clicq, R. W. Tjerkstra, J. G. E. Gardeniers, A. v. d. Berg, G. V. Baron and G. Desmet, *Journal of Chromatography A*, 2004, 1032, 185-191.
5. W. D. Malsche, D. Clicq, V. Verdoold, P. Gzil, G. Desmet and H. Gardeniers, *Lab on a Chip*, 2007, 7, 1705-1711.
6. W. D. Malsche, H. Gardeniers and G. Desmet, *Analytical Chemistry*, 2008, 80, 5391-5400.
7. R. M. Tiggelaar, V. Verdoold, H. Eghbali, G. Desmet and J. G. E. Gardeniers, *Lab on a Chip*, 2008, 9, 456-463.
8. N. V. Lavrik, L. C. Taylor and M. J. Sepaniak, *Lab on a Chip*, 2010, 10, 1086-1094.
9. C. E. Freye, N. A. Crane, T. B. Kirchner and M. J. Sepaniak, *Analytical Chemistry*, 2013, 85, 3991-3998.
10. J. M. F. Ceiler, P. A. Kohl and S. A. Bidstrup, *Journal of the Electrochemical Society*, 1995, 142, 2067-2071.
11. P.-z. Yang, L.-m. Liu, J.-h. Mo and W. Yang, *Semiconductor Science and Technology*, 2010, 25.
12. N. V. Lavrik, L. T. Taylor and M. J. Sepaniak, *Analytica Chimica Acta*, 2011, 694, 6-20.
13. L. C. Taylor, T. B. Kirchner, N. V. Lavrik and M. J. Sepaniak, *Analyst*, 2012, 137, 1005-1012.
14. O. Reynolds, *Proceedings of the Royal Society of London*, 1883, 35, 84-99.
15. G. Deininger, *Chromatographia*, 1976, 9.
16. A. B. D. Cassie and S. Baxter, *Transactions of the Faraday Society*, 1944, 40, 546-551.
17. H. Kusumaatmaja, C. M. Pooley, S. Girardo, D. Pisignano and J. M. Yeomans, *Physical Review E*, 2008, 77.
18. K. Tsougeni, D. Papageorgiou, A. Tserepi and E. Gogolides, *Lab on a Chip*, 2009, 10, 462-469.
19. R. N. Wenzel, *Industrial and Engineering Chemistry*, 1936, 28, 988-994.
20. G. Guiochon and S. Antoine, *Journal of Chromatographic Science*, 1978, 16, 470-481.
21. J. M. Miller, *Chromatography: Concepts and Contrasts*, John Wiley & Sons, Inc., Hoboken, NJ, 2005.
22. C. F. Poole, *Journal of Chromatography A*, 2003, DOI: 10.1016 /S0021-9673(03)00435-7, 963-984.
23. C. F. Poole, *The Essence of Chromatography*, Elsevier Science B.V., Amsterdam, 2003 edn., 2003.
24. S. K. Poole and C. F. Poole, *Journal of Chromatography A*, 2011, 1218, 2648-2660.
25. P. S. Variyar, S. Chatterjee and A. Sharma, in *High-Performance Thin-Layer Chromatography (HPTLC)*, ed. M. Srivastava, Springer, 2011, ch. 2.
26. S. R. Jim, A. J. Oko, M. T. Taschuk and M. J. Brett, *Journal of Chromatography A*, 2011, 1218, 7203-7210.
27. R. D. Deegan, O. Bakajin, T. F. Dupont, G. Huber, S. R. Nagel and T. A. Witten, *Nature*, 1997, 389.
28. B. M. Weon and J. H. Je, *Physical Review*, 2010, 82.